

Fabrication of Resorcinol-Formaldehyde Xerogel based High Aspect Ratio 3-D Hierarchical C-MEMS Structures

C. S. Sharma^a, H. Katepalli^b, A. Sharma^b, G. T. Teixidor^c and M. J. Madou^c

^a Department of Chemical Engineering, Indian Institute of Technology Hyderabad, Yeddumailaram, AP 502205, INDIA

^b Department of Chemical Engineering and DST Unit on Soft Nanofabrication, Indian Institute of Technology Kanpur, UP 208016, INDIA

^c Department of Mechanical & Aerospace & Biomedical Engineering, University of California, Irvine, CA 92697, USA

We demonstrate a novel method to fabricate arrays of resorcinol-formaldehyde xerogel (RFX) based high aspect ratio (HAR) three-dimensional (3-D) hierarchical C-MEMS structures. Starting from a master pattern of HAR 3-D posts fabricated in SU-8 negative photoresist by photolithography, a negative PDMS stamp with arrays of holes was prepared by micromolding. The PDMS stamp was then used to fabricate HAR 3-D RFX posts by replica molding. The 3-D RFX posts thus fabricated were electrosprayed with SU-8 or an RF sol in the form of submicron or nano sized droplets and followed by pyrolysis to yield HAR 3-D hierarchical carbon posts. To characterize their use in C-MEMS based batteries, galvanostatic (charge and discharge) experiments on RFX derived carbon showed that it can be reversibly intercalated with Li ions and possesses superior intercalation properties as compared to SU-8 derived carbon which is a widely used material in C-MEMS.

Introduction

In order to meet future energy demands, improvement of Li ion battery technology in terms of specific capacity, power, manufacturing cost, safety and sustainability are important research goal (1-5). Possible strategies to improve Li ion battery technology include developing new active electrode materials (anode and cathode), better separators and electrolytes, and reconsidering the basic architecture of these batteries (1-26). In commercial Li ion batteries, carbon materials are primarily being used as anodes (1, 2, 4, 8, 10-29). There are two broad categories of carbon materials; soft (graphitic) and hard (non-graphitic) carbon. Advantages and disadvantages associated with either type of carbon materials for use in Li-ion batteries are discussed elsewhere (3, 18-20, 27, 28). Resorcinol-formaldehyde (RF) based porous carbon aerogels, first introduced by Pekala (30) in 1989 have been studied as anode materials in batteries and supercapacitors (23-25). Activated carbon, carbon nanotubes, glassy carbon and many carbon allotropes have been investigated as potential electrode materials (3, 12, 18, 19, 26). Although many new anode materials have been researched over the years, fewer attempts have been made to rethink the electrode design (4-14). In one of those redesign efforts geared towards achieving enhanced power and energy density, it was demonstrated that 3-D electrode architecture is more useful than the conventional thin film (2-D) approach (4, 6-11). This

can be attributed to the reduced ionic transport distances and the accommodation of more active electrode material in the same footprint in a 3-D architecture compared to a thin film format (6, 7, 9). A wide variety of methods are currently being explored for the fabrication of 3-D electrode arrays (4, 7, 8, 10, 11), the most promising of which has been direct photo-patterning and pyrolysis of SU-8 photoresist. Recently, Madou *et al.* (13,14) demonstrated mathematically that a fractal electrode design constitutes a more optimal design for energy conversion devices because of the maximization of electrochemically active surface area while minimizing the electrical work involved. However, the fabrication of a truly 3-D multiscale or fractal carbon electrodes remains a challenging task.

In this study, we used resorcinol-formaldehyde xerogel (RFX) (23-25, 30, 31) as an organic precursor to yield non-porous dense carbon. We demonstrate the ease of fabrication of high aspect ratio (HAR) RFX 3-D structures by replica molding. We show that both the material (RF gel) and the fabrication method (micromolding and electrospaying) used here for 3-D Li battery architecture are superior to the fabrication of micro-post arrays by SU-8 using photolithography. Further, we fabricated arrays of carbon hierarchical microposts using a combination of top-down (replica molding) and bottom-up (electrospaying) manufacturing approaches. Finally, we show that RFX derived non-porous dense carbon films can be reversibly charged and discharged with Li ions and thus may be a potential contender as anode materials for 3-D microbattery architecture.

Experimental

We first fabricated 3-D micro-arrays of SU-8 by photopatterning using standard photolithography. SU-8 is a negative photoresist that yields glassy carbon upon pyrolysis and this carbon can be reversibly intercalated with Li ions. Madou *et al.* demonstrated the use of SU-8 photoresists to fabricate high aspect ratio pillars by photolithography (4, 8, 10, 11). One can achieve aspect ratios as high as 20 by this top-down method (8, 10, 11). These SU-8 HAR structures on Si wafers were then used as a master stamp. A mixture of a PDMS elastomer and a curing agent (supplied by Dow Chemicals) in a 10:1 weight ratio was prepared and cast over these master stamps for making negative replicas. These replicas were cured at 120°C for 12 h in an oven and after curing and cooling; the PDMS replicas were gently peeled off the master stamps.

RFX was synthesized by the polycondensation of resorcinol and formaldehyde in an organic solvent (acetone) in the presence of an acidic catalyst (hydrochloric acid). All the chemicals used in preparation of RFX were purchased from Qualigens Fine Chemicals, India. First a clear solution of Resorcinol (2.0 gm) and Formaldehyde (2.5 ml) was prepared by stirring magnetically for about 15 min. A separate solution of acetone (30 ml) and hydrochloric acid (0.7 ml) was prepared and mixed with the RF clear solution. After stirring this mixture for about 10 min, a light pink colored RF sol is formed. The RF sol was then poured into the PDMS template and stored at room temperature for 24 h to reach the sol gelation stage. Once the RF sol becomes solid and changes to a dark brown color, the PDMS stamp was carefully peeled off without destroying any of the resulting patterns. The patterned RF gel HAR structures were dried in a controlled environment as in the scheme shown below to allow for their isotropic shrinkage without cracking (Figure 1a). These drying conditions optimized for isotropic crack free shrinkage are as follows: At room temperature (~ 30 °C) for 24 h; At 50 °C for 12h; At 60 °C for 12 h; At 80 °C for 6h; At 120 °C for 2h.

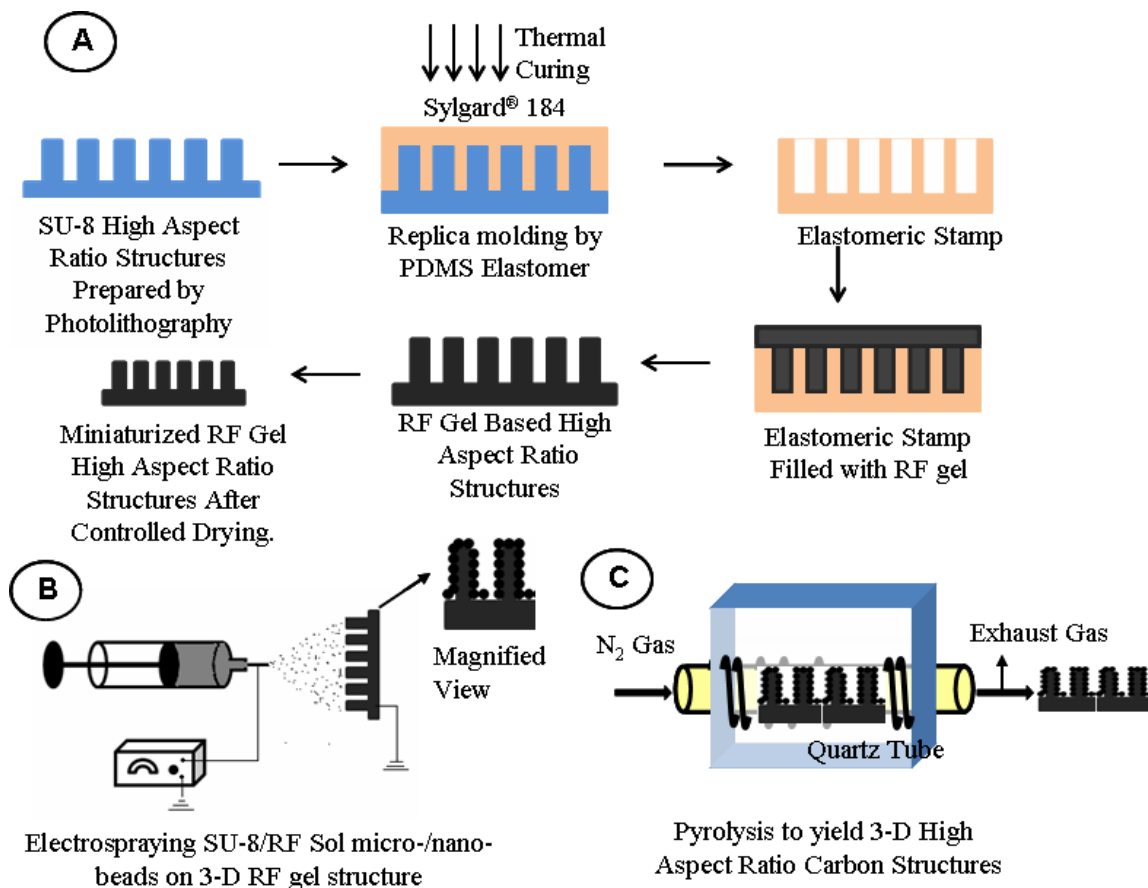


Figure 1. Schematic of the (a) fabrication of RFX based HAR 3-D posts; (b) deposition of SU-8 or RFX based submicron and nano droplets on RFX based 3-D posts by electro spraying to make hierarchical structures; (c) pyrolysis to yield an array of RFX derived HAR 3-D hierarchical carbon posts

To obtain the desired hierarchical carbon structures, we used electro spraying on RFX based 3-D microarrays as shown in the schematic in Figure 1b). During electro spraying a polymer spray is ejected towards a collector screen from a spraying syringe filled with polymer solution by applying a high voltage between syringe and substrate. The electro spraying set up was homebuilt and details of this set-up were reported in previous papers (31, 32).

SU-8 photoresist (SU-8 2002; viscosity 7 cSt at 25°C) (MicroChem Corp. USA) was electro sprayed to deposit sub-micron beads while RF sol was electro sprayed in the form of nano-sized droplets. We have shown that by fine tuning the electro spinning parameters, one can get a variety of RF morphologies including fibers, beaded fibers and isolated beads only (32). The conditions reported here were specifically optimized for obtaining beads (31, 32). More details on the optimization of electro spinning parameters for RF sol can be found in our work reported elsewhere (31, 32).

After conformal deposition of SU-8 or RF sol based submicro- and nano- beads respectively on the high aspect ratio 3-D RFX structures, the entire integrated constructs were pyrolyzed in an inert atmosphere to yield HAR 3-D hierarchical carbon structures (Figure 1c). The pyrolysis conditions were as follows: from room temperature to 300°C

with linear ramping in 3 h; At 300°C for 1 h; From 300°C to 900°C in 2 h; At 900°C for 1 h.

The above process was followed by naturally cooling over nearly 12 h while maintaining a constant nitrogen flow rate of 0.2 lpm throughout the process.

Electrochemical measurements

An RF sol, prepared as described above, was spin coated onto a Si wafer (with an oxide layer of 500 nm) at 3000 rpm for 20 s to fabricate thin films. Drying and pyrolysis conditions were the same as we described above. The RFX derived carbon films so obtained were used as working electrodes while a Li foil (0.75 mm thick, 99.9% purity, Aldrich) was used as counter electrode in an electrochemical cell. The electrolyte used was a 1M solution of lithium perchlorate (95% purity, Aldrich) in a 1:1 (v/v) mixture of ethylene carbonate (Anhydrous, 99%, Aldrich) and dimethyl carbonate (99% purity, Aldrich). An electrochemical test cell made of Teflon was designed with an effective working electrode area of 0.654 cm². Galvanostatic (charge and discharge) experiments were performed at two different current densities 76.4 and 152.7 μA cm⁻² at between 0.05 and 3.0 V using a multichannel potentiogalvanostat (Gamry Instruments). Soaking time of 2 hours was maintained for all the test samples. Thickness of RFX derived carbon films were measured using surface profilometer (Tencor Alpha Step 200). Specific and gravimetric capacities as reported later were calculated as follows:

Specific capacity = current (mA) x time (h) / area of the electrode (cm²)

Gravimetric Capacity = (specific capacity) / (density (gcm⁻³) x thickness (cm))

Results and Discussion

The C-MEMS electrode fabrication process starts with an array of 3-D SU-8 cylindrical posts (aspect ratio ~6, width ~ 25 micron) as a master pattern for replica molding (Figure 2a). Fabrication of these original SU-8 HAR 3-D posts is based on photolithography as reported elsewhere (8, 10, 11). A PDMS stamp, as shown in Figure 2b, was then prepared by replica molding using this SU-8 master pattern. In the next step, this negative PDMS replica was used as a master to create an array of 3-D RFX microposts as illustrated in Figure 2c. By controlling the molding process parameters (as detailed in the experimental section), the fidelity of the printing pattern can be maintained adequately. Thus with a proper control of conditions, replica molding is demonstrated to be an effective route for fabrication of 3-D structures in RFX over a large area. This pattern can be subsequently pyrolyzed to obtain an array of HAR carbon posts (Figure 2d). The carbon yield of RFX was nearly 50%. In this manner it is easy to produce a large number of HAR 3-D RFX posts over large surface areas using a single SU-8 master pattern without the need of UV lithography every time SU-8 derived carbon post arrays are required in 3-D microbattery mass manufacture. Besides fabricating round posts, we have also used a cross shaped design (aspect ratio ~4, width ~50 micron) for the 3-D posts (Figure 2e). It was recently demonstrated that cross shaped high aspect ratio posts retain their integrity better upon pyrolysis as compared to cylindrical posts which aggregate rather readily due to capillary effects (4). The PDMS replicas (Figure 2f) retain the cross shaped structures with high fidelity and were again used as the master for making 3-D structures from the RF gel.

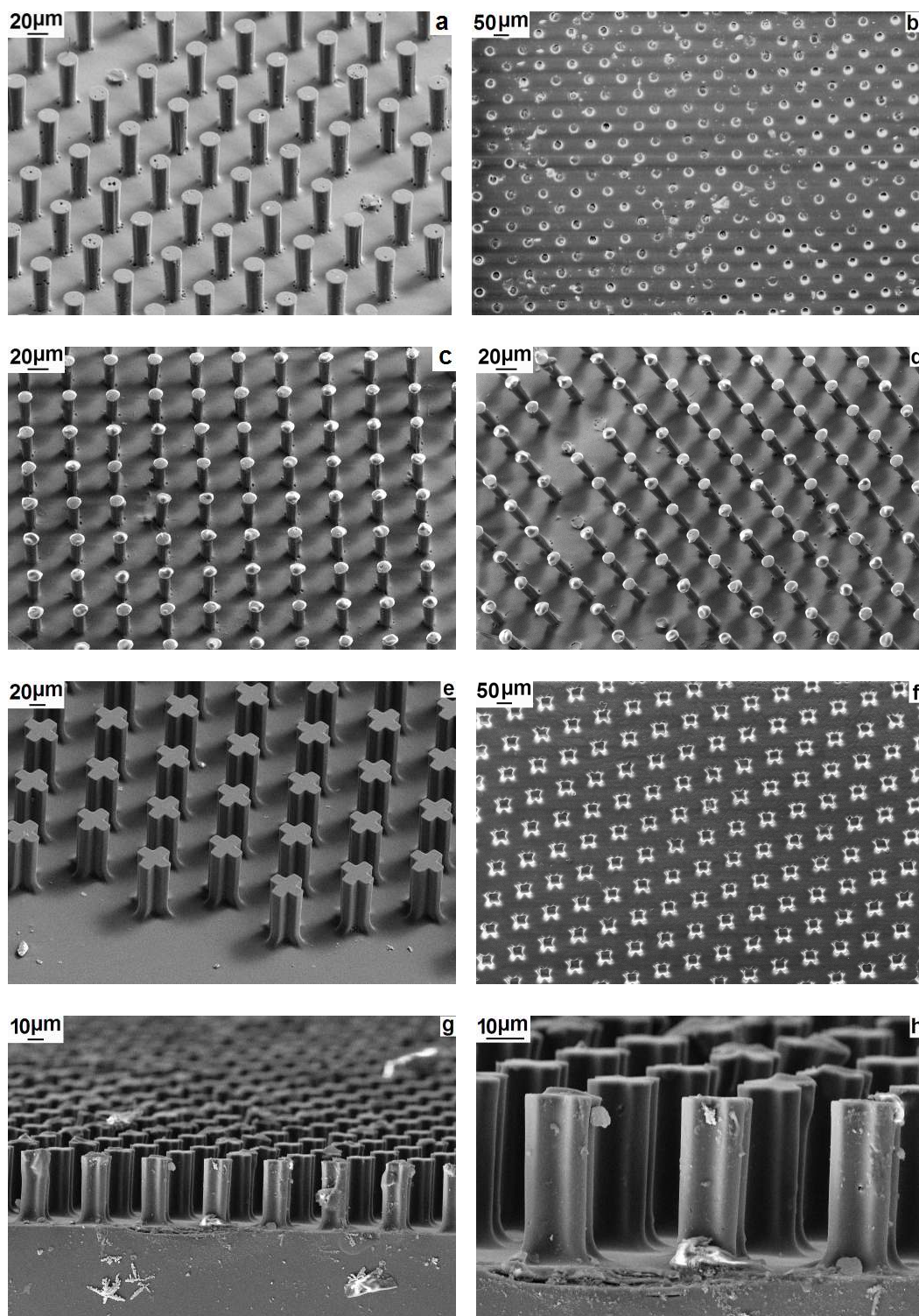


Figure 2. (a) HAR 3-D cylindrical posts in SU-8 used as master pattern; (b) PDMS replica showing holes; (c) RFX based cylindrical posts; (d) RFX derived cylindrical non-porous carbon posts; (e) HAR 3-D posts with cross shaped design in SU-8; (f) PDMS replica showing holes; (g)-(h) RFX derived 3-D cross shaped non-porous carbon posts

It is important to note that during the conditions of drying employed here, RFX shrinks isotropically (33), thus maintaining the aspect ratio of the 3-D RFX posts very close to that of the original SU8 master stamp. However, the absolute dimensions of the

posts (diameter and height) are reduced by nearly 60% of the original SU-8 pattern. A further shrinkage (~10%) was observed during pyrolysis.

After the successful fabrication of RFX derived HAR 3-D carbon posts, we further integrated these microstructures with sub-micron and nano-scale carbon beads to fabricate multiscale, fractal-like hierarchical carbon structures. Conformal deposition of micro and nano particles over the array of RFX based microposts was carried out by electro spraying SU-8 photoresist or RF sol. Electro spraying and electro spinning are established techniques to prepare nanostructures with various morphologies (fibres, beaded fibres and beads) on a collector surface. The exact type of nanostructure depends on the process and solution parameter details. In electro spraying, a jet of polymer solution issues from a nozzle by applying a high voltage between the nozzle and a substrate. The high voltage allows for the elongation of the liquid meniscus at the nozzle opening to form a jet which finally disrupts into fine droplets (in electro spraying) or fibers (in electro spinning). In previous work, we optimized the various process parameters involved in the electro spraying of SU-8 and RF sols to form roughly monodisperse carbon sub-micron and nano- spheres (31, 32).

After electro spraying, the polymer post arrays covered with polymer beads were pyrolyzed to form HAR 3-D carbon posts covered with sub-micron and nano sized carbon beads as shown in Figure 3. Figure 3a-c shows the conformal nature of the deposition of SU-8 derived carbon submicron spheres (average diameter 275.4 ± 83.1 nm) on the cross-shaped carbon posts. A magnified view of a side and a top of a cross-shaped post clearly demonstrates that this novel approach to fabricate hierarchical structures is quite efficient in covering complex 3D substrates. Similarly, RFX derived electro sprayed carbon nanospheres (average diameter 72.5 ± 21.2 nm) were deposited on RFX derived 3-D carbon posts (Figure 3d-f). Cylindrical posts were also integrated with SU-8 derived submicron carbon spheres to obtain an array of hierarchical carbon posts as shown in Figure 3g-i.

Thus, replica molding using RFX is easy and cost effective for the fabrication of large area, multiple samples of high aspect ratio arrays of carbon micro-posts as compared to photolithography of SU-8 photoresist. Additionally by electro spraying, we were able to fabricate arrays of hierarchical carbon posts also which have higher external surface area.

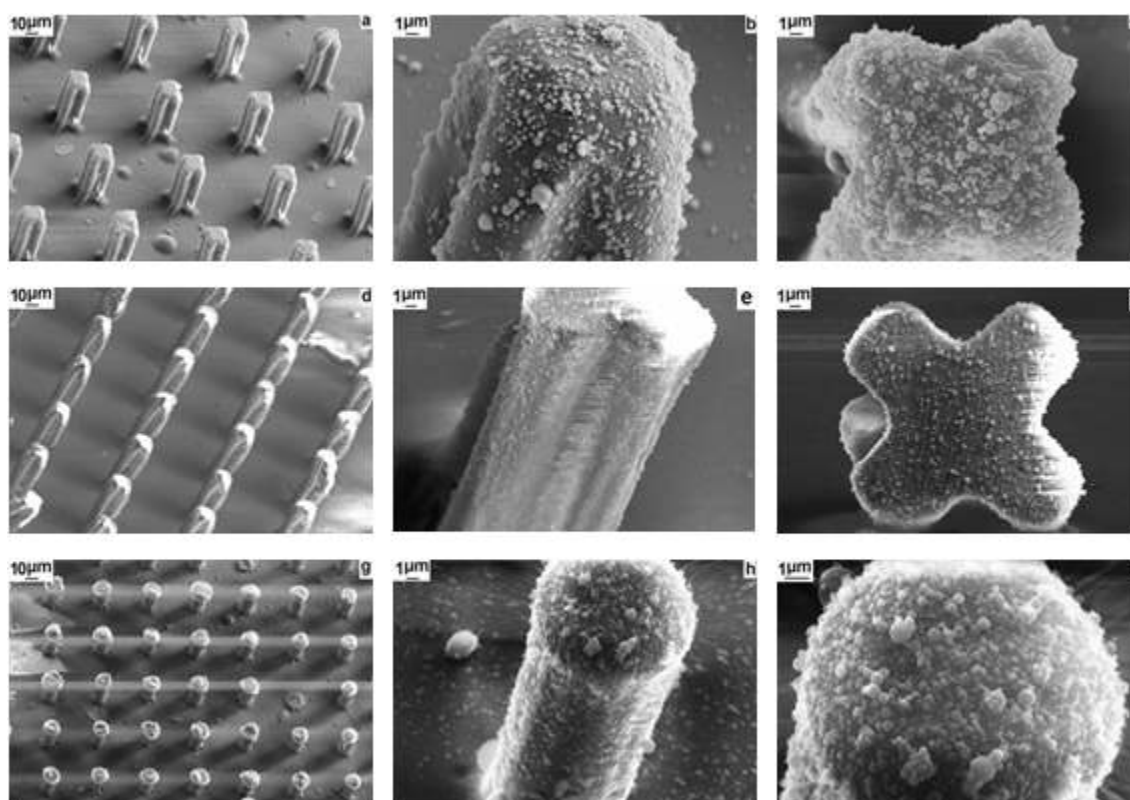


Figure 3. (a) An array of RFX derived cross shaped carbon posts integrated by electrospayed SU-8 derived submicron size carbon spheres; (b) magnified side view of a post; (c) magnified view of top of the one of the posts showing a conformal deposition of submicron carbon spheres; (d) an array of RFX derived cross shaped carbon posts integrated by electrospayed RFX derived carbon nanospheres; (e) magnified side view of a post; (f) magnified view of top of the one of the posts showing a conformal deposition of carbon nanospheres; (g) an array of RFX derived cylindrical carbon posts integrated by electrospayed SU-8 derived submicron size carbon spheres; (h) magnified side view of such a hierarchical post; (i) magnified view of top of the one of the cylindrical posts showing a dense conformal deposition of submicron carbon spheres

Further, in order to establish the use of RFX derived 3-D hierarchical arrays of non-porous carbon microposts in C-MEMS batteries, the electrochemical behavior of RFX derived non-porous dense carbon films were tested galvanostatically as shown in Figure 4. The pyrolyzed RFX exhibited reversible intercalation-deintercalation of lithium as demonstrated in Figure 4.

Figure 4a shows first six charge/discharge cycles at a constant current density of $76.4 \mu\text{A cm}^{-2}$. The reason the discharge capacity in the first cycle is much larger than in subsequent cycles can be attributed to the formation of a solid electrolyte interphase (SEI) layer on the electrode surface (29). SEI film forms due to the electrochemical reduction of electro-active species present in the electrolyte and it is widely recognized that the presence of this film plays a very important role in battery performance (29). For the next five cycles we observe that the discharge capacity remains nearly constant. This type of cycling behavior is consistent with the behavior observed for the traditional coke materials used as lithium electrode materials (8, 10, 11). Figure 4b and 4c illustrate a

comparison of gravimetric and specific capacities of RFX derived carbon with SU-8 photoresist derived carbon at two different current densities evaluated based on the working electrode area ($76.4 \mu\text{A cm}^{-2}$ and $152.7 \mu\text{A cm}^{-2}$). The mass of the active carbon material was 0.194 mg while the thickness of the RFX derived carbon films was measured to be $1.748 \mu\text{m}$. The reversible capacity of the RF gel derived carbon at a current density of $76.4 \mu\text{A cm}^{-2}$ was found to be 195.1 mAh/g which is similar to that of SU-8 derived carbon ($\sim 220 \text{ mAh/g}$) (11). Similarly at a current density of $152.7 \mu\text{A cm}^{-2}$ also, the reversible capacity for RFX and SU-8 derived carbon (4) was found to be nearly equal (160.0 and 180.1 mAh/g respectively). Columbic efficiency as defined by ratio of discharge to charging capacity was calculated to be more than 90% for any given cycle. We further calculated the irreversible capacity as the difference between the first and sixth charge cycle at a current density of $76.4 \mu\text{A cm}^{-2}$. For RFX derived carbon, it was found to be 213.6 mAh/g which was significantly less than 304.2 mAh/g as reported for SU-8 derived carbon (4). Next, we calculated the reversible and irreversible specific capacities as shown in Figure 4c. At both current densities ($76.4 \mu\text{A cm}^{-2}$ and $152.7 \mu\text{A cm}^{-2}$), these values were found to be close to those for RFX and SU-8 derived carbon^[4] (0.058 and 0.048 mAh/cm^2 respectively). However for RFX derived carbon, the irreversible specific capacity was found to be significantly less (0.0636 mAh/cm^2) than what has been for SU-8 derived carbon (4) (0.0788 mAh/cm^2). In other words, irreversible capacity was found to be 9.5% as compared to $\sim 40\%$ for SU-8 derived carbon. For graphite also, irreversible capacity is normally below 10% . It is to be noted that percentage irreversible capacity was calculated as follows: $[\% = (\text{irrev.} - \text{rev.}) / \text{rev.} \times 100]$. These results establish that RFX derived carbon can not only be charged and discharged with Li ion, but also shows less irreversible capacity compared to SU-8 derived carbon. Percentage irreversible capacity losses were found to be similar to that of graphite. Therefore, RFX derived carbon has potential to be used as an anode material in energy storage devices including Li ion battery.

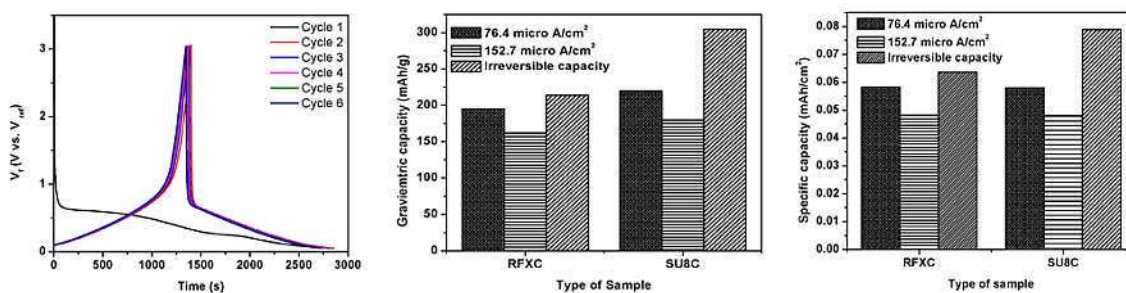


Figure 4: (a) Galvanostatic charge/discharge cycle behavior of RF gel derived carbon film for first six cycles; (b) comparison of gravimetric capacity of RFX derived carbon with SU-8 derived carbon; (c) comparison of specific capacity of RFX derived carbon with SU-8 derived carbon. The reported values for capacities in (b) and (c) are after 20 cycles.

Conclusions

We have introduced RFX as a polymer precursor to the fabrication of complex carbon shapes through pyrolysis including arrays of high aspect ratio 3-D carbon micro posts. By using soft lithography in the fabrication process, we avoid the use of UV lithography equipment each time a new batch of 3D carbon structures are to be made. We also

developed a simple and novel method to integrate polymer nano-spheres with these RFX posts by electro spraying, yielding a 3-D high aspect ratio hierarchical array of carbon posts upon pyrolysis. As these hierarchical carbon structures have high external surface area, these structures can be very useful in various applications where a high surface area is desirable such as in energy storage devices and sensing devices. To enable their use in C-MEMS batteries, we have shown that RFX derived carbon can be reversibly intercalated with Li ions. We further compared the electrochemical performance of RFX derived carbon with SU-8 derived carbon, a material used in C-MEMS batteries. Interestingly, RFX derived carbon not only shows similar values for the reversible gravimetric and specific capacities as that of SU-8 derived carbon but shows a significant reduction in irreversible capacity compared to SU-8 (percentage irreversible capacity similar to graphitic carbon electrode). These results indicate that RFX derived carbon has excellent electrochemical properties and therefore could be an important contender as an anode material for Li ion batteries. The ability to easily and inexpensively pattern arrays of 3-D hierarchical carbon structures opens up a wide range of possibilities for researchers to develop various new electrodes for energy storage devices and sensors.

Acknowledgements

This work was supported by the DST Unit on Soft Nanofabrication at IIT Kanpur and the Indo-US Center of Excellence in Fabricionics. Helpful discussions with Dr. Manish Kulkarni are greatly acknowledged.

References

1. M. Armand and J. -M. Tarascon, *Nature*, **451**, 652 (2008).
2. M. Winter and R. J. Brodd, *Chem. Rev.*, **104**, 4245 (2004).
3. A. K. Shukla and T. P. Kumar, *Curr. Sci.*, **94**, 314 (2008).
4. G. T. Teixidor, R. B. Zaouk, B. Y. Park and M. J. Madou, *J. Power Sources*, **183**, 730 (2008).
5. R. E. Garcia, Y. M. Chiang, W. C. Carter, P. Limthongkul and C. M. Bishop, *J. Electrochem. Soc.*, **152**, A255 (2005).
6. R. W. Hart, H. S. White, B. Dunn and D. R. Rolison, *Electrochem. Commu.*, **5**, 120 (2003).
7. J. W. Long, B. Dunn, D. R. Rolison and H. S. White, *Chem. Rev.*, **104**, 4463 (2004).
8. C. Wang, L. Taherabadi, G. Jia, M. Madou, Y. Yeh, and B. Dunn, *Electrochem. Solid- State Lett.*, **7**, A435 (2004).
9. R. E. Garcia and Y-M. Chiang, *J. Electrochem. Soc.*, **154**, A856 (2007).
10. C. Wang and M. Madou, *Biosensors and Bioelectronics*, **20**, 2181 (2005).
11. C. Wang, G. Jia, L. H. Taherabadi and M. Madou, *J. MEMS.*, **14**, 348 (2005).
12. O. J. A. Schueller, S. T. Brittain, C. Marzolin and G. M. Whitesides, *Chem. Mater.*, **9**, 1399 (1997).
13. B. Y. Park, R. Zaouk, C. Wang and M. Madou, *J. Electrochem. Soc.*, **154**, P1 (2007).
14. G. T. Teixidor, B. Y. Park, P. P. Mukherjee, Q. Kang and M. Madou, *Electrochimica Acta*, **54**, 5928 (2009).
15. J. Kim, X. Song, K. Kinoshita, M. Madou, and R. White, *J. Electrochem. Soc.*, **145**, 2314 (1998).

16. H. Fujimoto, A. Mabuchi, K. Tokumitsu and T. Kasuh, *J. Power Sources*, **54**, 440 (1995).
17. M. Winter, J. O. Besenhard, M. E. Spahr and P. Novak, *Adv. Mater.*, **10**, 725 (1998).
18. S. Flandrois and B. Simon, *Carbon*, **37**, 165 (1999).
19. M. Endo, C. Kim, K. Nishimura, T. Fujino and K. Miyashita, *Carbon*, **38**, 183 (2000).
20. E. Buiel and J. R. Dahn, *Electrochimica Acta*, **45**, 121 (1999).
21. R. Alcantara, F. J. F. Madrigal, P. Lavela, J. L. Tirado, J. M. L. Mateos, C. G. Salazar, R. Stoyanova, and E. Zhecheva, *Carbon*, **38**, 1031 (2000).
22. J. Yao, G. X. Wang, J. Ahn, H. K. Liu and S. X. Dou, *J. Power Sources*, **114**, 292 (2003).
23. R. Alcantara, P. Lavela, G. F. Ortiz and J. L. Tirado, *Electrochem. Solid State Lett.*, **8**, A222 (2005).
24. Y. Zhu, H. Hu, W. Li and X. Zhang, *Carbon*, **45**, 160 (2007).
25. L. Zhang, H. Liu, M. Wang and L. Chen, *Carbon*, **45**, 1439 (2007).
26. Y. Wang, F. Su, C. D. Wood, J. Y. Lee and X. S. Zhao, *Ind. Eng. Chem. Res.*, **47**, 2294 (2008).
27. W. Xing and J. R. Dahn, *J. Electrochem. Soc.*, **144**, 1195 (1997).
28. J. R. Dahn, T. Zheng, Y. Liu, and J. S. Xue, *Science*, **270**, 590 (1995).
29. F. Galobardes, C. Wang and M. Madou, *Diamond & Related Mater.*, **15**, 1930 (2006).
30. R. W. Pekala, *J. Mater. Sci.*, **24**, 32221 (1989).
31. C. S. Sharma, S. Patil, S. Saurabh, A. Sharma and R. Venkataraghavan, *Bull. Mater. Sci.*, **32**, 239 (2009).
32. C. S. Sharma, R. Vasita, D. K. Upadhyay, A. Sharma, D. S. Katti and R. Venkataraghavan, *Ind. Eng. Chem. Res.*, **49**, 2731 (2010).
33. C. S. Sharma, A. Verma, M. M. Kulkarni, D. K. Upadhyay and A. Sharma, *ACS Appl. Mater. Inter.*, **2**, 2193 (2011).